Adsorption 11: 37–42, 2005

Prediction of Adsorption of Nonideal Mixtures in Nanoporous Materials

ALAN L. MYERS
Chemical and Biomolecular Engineering, University of Pennsylvania, Philadelphia, Pennsylvania, 19104, USA
amyers@seas.upenn.edu

Abstract. The prediction of multicomponent adsorption equilibria from single-component adsorption experiments is a challenging and important problem. Predictions based upon the assumption of an ideal adsorbed solution (IAS) may give unacceptable errors, especially in the case of large differences in the size or the polarity of the adsorbate molecules. These differences in molecular properties generate differences in the chemical potential of the solid (ψ) that may be used to predict activity coefficients for nonideal adsorbed solutions (NIAS). The ψ plots for pure-gas isotherms identify ideal solutions and provide reliable predictions of mixture equilibria for nonideal adsorbed solutions.

Keywords: adsorption, nanopores, ideal, nonideal, mixtures

Introduction

The assumption of an ideal adsorbed solution (Myers and Prausnitz, 1965) provides a thermodynamically consistent method of predicting mixture equilibria from single-gas adsorption isotherms of any mathematical form. The problem is that one cannot decide in advance which mixtures are ideal. Although there is a strong correlation between nonideal adsorbed solutions and the differential enthalpies of the pure gases (Siperstein and Myers, 2001), accurate enthalpy data are usually unavailable.

New Definition of Ideal Adsorbed Solution (IAS)

Single-component adsorption is actually a binary mixture; binary adsorption is actually a ternary mixture. Therefore it should be possible to define an "activity coefficient" for the interaction of the solid with a pure gas. Since the gas and solid in which it adsorbs are in different states, the standard methods of solution thermodynamics for the definition of activity coefficients do not apply.

The chemical potential of the solid is the grand potential of adsorption Ω (Myers, 2002):

$$\Omega = -RT \int_0^P \frac{n}{P} dP \quad \text{(constant } T\text{)} \tag{1}$$

The reference state for the chemical potential is the clean adsorbent *in vacuo*. Define:

$$\psi = -\frac{\Omega}{RT} \tag{2}$$

ψ is a positive variable with the same units (mol kg^{-1}) as the amount adsorbed. An ideal adsorbed solution is one for which the chemical potentials of the solid are the same for the individual pure components. Two gases with equal values of ψ interact with the surface in the same way and therefore their adsorbed solution must be ideal. Figure 1 shows an example for ethylene and ethane adsorbed on Nuxit activated carbon (Szepesy and Illes, 1963). The reduced chemical potentials of the solid coincide (within 2%) for adsorption of the individual gases and their adsorbed solution is ideal (within 2%) as shown on Fig. 2.

Effect of Energetic Heterogeneity

If ideal adsorbed solutions have equal values of ψ, then the degree of nonideality of an adsorbed mixture should be proportional to the difference $\Delta\psi$ for the pure components.

Any model of heterogeneity for the gas-solid interaction energy requires a choice for its distribution. The

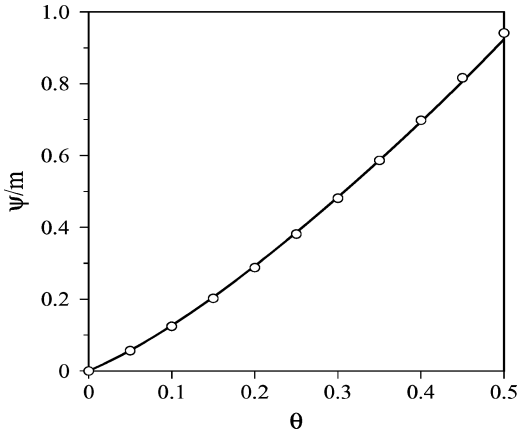

Figure 1. ψ plot for adsorption of pure gases on activated carbon at 20°C. —: C_2H_6. ○: C_2H_4.

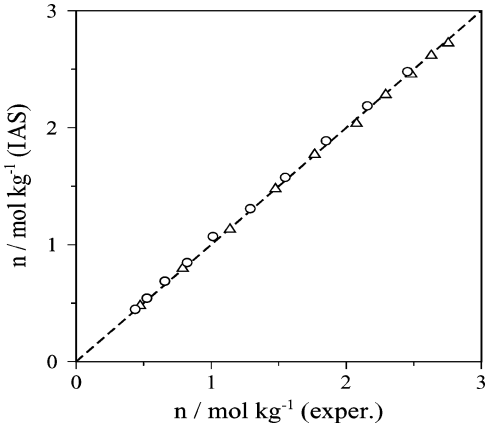

Figure 2. Comparison of IAS with experiment for binary adsorption on Nuxit activated carbon at 20°C. △: C_2H_6; ○: C_2H_4.

symmetrical beta distribution is chosen here because of its flexibility, which ranges from a uniform distribution (no. 1 on Fig. 3) to a Gaussian-like distribution (no. 3 on Fig. 3). A discrete distribution with two energies (no. 4 on Fig. 3) is also shown. All four distributions have equal values for their average and standard deviation. Assuming Langmuir's equation for each gas-solid interaction energy, the adsorption isotherms for pure components and mixtures may be written as integrals over the energy distribution:

$$n_1(P, y_1) = \frac{m_1\Gamma(2a)}{[\Gamma(a)]^2}\int_0^1 \left(\frac{C_1(z)Py_1}{1+C_1(z)Py_1+C_2(z)Py_2}\right) \times [z(1-z)]^{a-1}dz \quad (3)$$

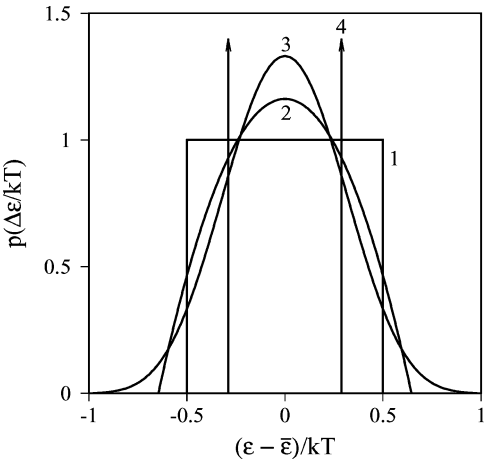

Figure 3. Distributions for energy of adsorption. (1): uniform ($a = 1$); (2): intermediate ($a = 2$); (3) Gaussian-like ($a = 10$); (4) discrete (two energies). $\sigma = 1/(2\sqrt{3})$ for all distributions.

$$n_2(P, y_2) = \frac{m_2\Gamma(2a)}{[\Gamma(a)]^2}\int_0^1 \left(\frac{C_2(z)Py_2}{1+C_1(z)Py_1+C_2(z)Py_2}\right) \times [z(1-z)]^{a-1}dz \quad (4)$$

where Γ is the gamma function and the parameter $a \geq 1$ determines the shape of the beta distribution as shown on Fig. 3. The chemical potential of the solid is:

$$\psi(P, y_1) = \frac{m_{12}\Gamma(2a)}{[\Gamma(a)]^2}\int_0^1 \ln[1 + C_1(z)Py_1 + C_2(z)Py_2][z(1-z)]^{a-1}dz \quad (5)$$

m_{12} is the harmonic mean of the capacities at pore filling for the individual components of the mixture:

$$\frac{1}{m_{12}} = \frac{1}{2}\left[\frac{1}{m_1} + \frac{1}{m_2}\right] \quad (6)$$

The constant C varies with the distribution of the gas-solid interaction energy:

$$C_i(z) = C_{oi}\exp[t_i(z - 0.5)] \quad (7)$$

The variable t depends upon the standard deviation (σ) and the shape (a) of the continuous distributions plotted on Fig. 3:

$$\sigma_i = \frac{t_i}{2\sqrt{2a+1}} \quad (8)$$

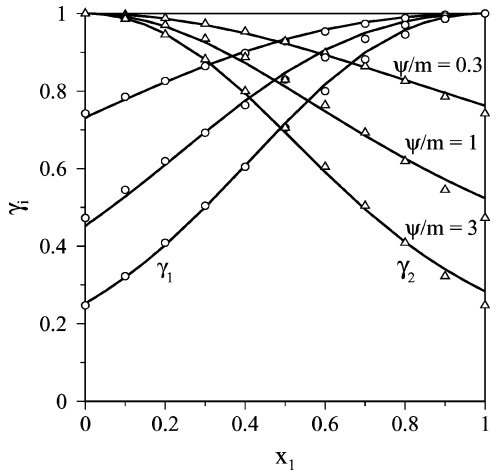

Figure 4. Activity coefficients for $\Delta\sigma = 2$, $a = 1$. Solid lines: Eq. (9). Points: symmetrical approximation, Eqs. (13) and (14).

Adsorbed-phase activity coefficients are defined by the deviation from ideality:

$$\gamma_i = \frac{Py_i}{P_i^\circ(\psi)x_i} \tag{9}$$

The activity coefficients calculated from these equations are functions of composition and ψ as shown on Fig. 4. Components with equal values of σ are ideal; the activity coefficients depend only on the *difference* in the standard deviations of the pure components. If the standard deviations of the two species are different, then the local selectivity will vary with the local energies and the mixture will become segregated, with a different composition at each position. The overall composition of the solution is:

$$x_1 = \frac{n_1}{n_1 + n_2} \tag{10}$$

Although the adsorbed solution is locally ideal, the energetic heterogeneity generates activity coefficients for the overall composition-averaged solution. It can be shown that $\gamma_i < 1$ except when both components have the same standard deviation, in which case Eqs. (3) and (4) reduce to Langmuir's equation for an ideal binary mixture.

The excess Gibbs free energy of mixing in the adsorbed phase is:

$$\frac{g^e}{RT} = x_1 \ln \gamma_1 + x_2 \ln \gamma_2 \tag{11}$$

Assume that g^e is quadratic in composition and symmetrical about $x = \frac{1}{2}$ so that:

$$\frac{g^e}{RT} = K(\psi)x_1x_2 \tag{12}$$

The activity coefficients are then:

$$\ln(\gamma_1) = K(\psi)x_2^2 \tag{13}$$

$$\ln(\gamma_2) = K(\psi)x_1^2 \tag{14}$$

Activity coefficients are compared with Eqs. (13) and (14) on Fig. 4. The agreement of theory with the quadratic approximation is good but the function $K(\psi)$ must still be determined. Define a reduced chemical potential $\psi_R = \psi/m$ at a reduced pore filling $\theta = (n/m) = \frac{1}{2}$ for single gas adsorption. Let component No. 1 have energetically heterogenous gas-solid interactions with $\sigma_1 > 0$ and let component no. 2 be energetically homogeneous so that $\sigma_2 = 0$. Remarkably, it can be shown that at the limit of pore filling:

$$\lim_{\psi\to\infty} K = -4\delta_{12} \tag{15}$$

exactly, where $\delta_{12} = |\psi_{1R} - \psi_{2R}|$ evaluated at $\theta = \frac{1}{2}$ as shown on Fig. 5. The value of δ_{12} increases with the standard deviation of the heterogeneous component. Eq. (15) is valid for all four distributions shown on

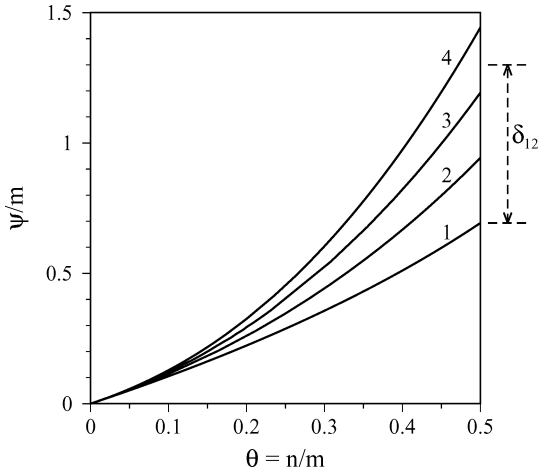

Figure 5. ψ plots. Reduced chemical potential of adsorbent for single-gas adsorption isotherms, $a = 1$. (1): $\sigma = 0$; (2): $\sigma = 1.52$; (3): $\sigma = 2.29$; (4): $\sigma = 2.96$.

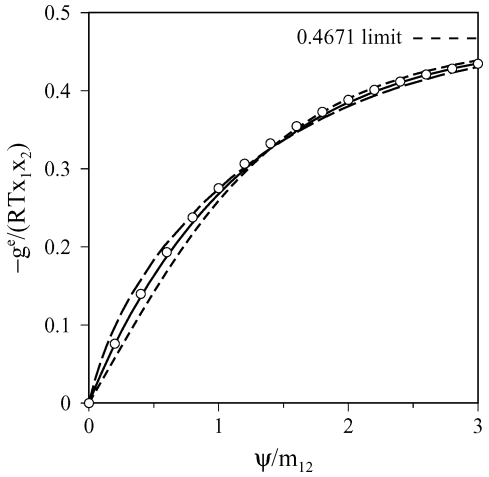

Figure 6. Variation of activity coefficients with ψ for $\Delta\sigma = 1$. Values of g^e at $x = \frac{1}{2}$. Long dashes: Gaussian; short dashes: discrete; solid line: uniform distribution. ○: Eq. (16).

Fig. 3 and applies to any symmetrical distribution of gas-solid energies.

At finite values of chemical potential, the activity coefficients depend upon the shape of the distribution as shown on Fig. 6. An approximate fit of all of these distributions is provided by:

$$\frac{g^e}{RT} = -4\delta_{12}\, x_1 x_2 [1 - e^{-\alpha_{12}\psi}] \qquad (16)$$

where $\alpha_{12} \equiv (1/m_{12})\exp(-\delta_{12})$. Equation (16) is plotted on Fig. 6 for comparison with the distributions shown on Fig. 3. In the Henry's law region of low pore filling where $\psi \to 0$, the limits are $g^e = 0$ and $\gamma_i = 1$ as required for an ideal solution. In the region of pore filling where $\psi \to \infty$, the limit $g^e/RT = -4\delta_{12}\, x_1 x_2$ applies to all symmetrical energy distributions.

Equation (16) enables the prediction of activity coefficients of nonideal adsorbed solutions (NIAS) using the constant δ_{12} extracted from single-gas adsorption isotherms. The activity coefficients are functions of ψ and adsorbed-phase composition:

$$\ln(\gamma_1) = -4\delta_{12}[1 - e^{-\alpha_{12}\psi}]x_2^2 \qquad (17)$$

$$\ln(\gamma_2) = -4\delta_{12}[1 - e^{-\alpha_{12}\psi}]x_1^2 \qquad (18)$$

The activity coefficients depend on the *difference* in standard deviations of the two components. The activity coefficients of a binary mixture with $\sigma_1 = 3$ and $\sigma_2 = 1$ are the same as the activity coefficients of a binary mixture with $\sigma_1 = 2$ and $\sigma_2 = 0$ because $\Delta\sigma$ is the same for both mixtures.

Comparison of NIAS with Simulations

Reduced chemical potentials for simulations of adsorption of nonpolar Lennard-Jones molecules in a spherical cavity (diameter 1.14 nm) are plotted on Fig. 7. The molecular diameters of the large and small molecules are 0.513 and 0.382 nm, respectively. At $\theta = 0.5$ on Fig. 7, $\delta_{12} = |\psi_{1R} - \psi_{2R}| = 0.202$. Activity coefficients from the simulation (Dunne and Myers, 1994) are compared with NIAS predictions on Fig. 8 and the agreement is almost perfect. These so-called entropic

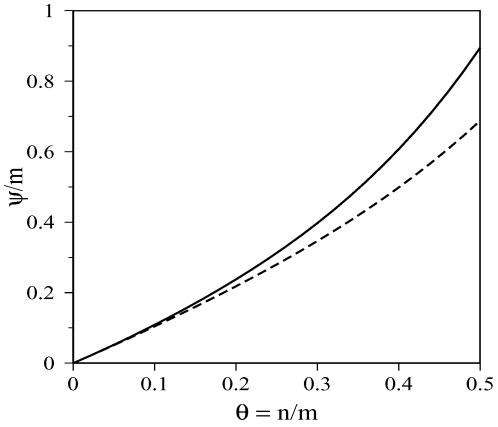

Figure 7. Simulated ψ plots at 50°C. Solid line: large molecule; dashed line: small molecule.

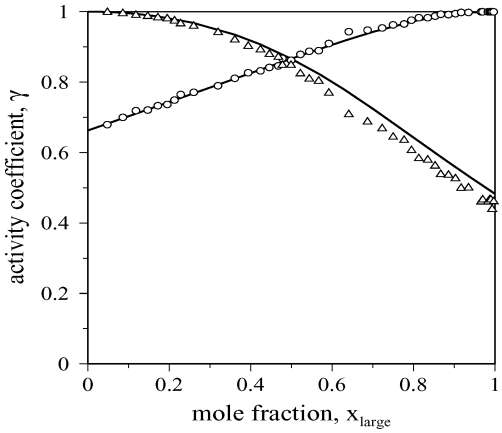

Figure 8. Activity coefficients at 50°C, 1000 kPa. Simulations: ○: large molecule; △: small molecule. Solid lines: NIAS, Eqs. (17) and (18), $\delta_{12} = 0.202$.

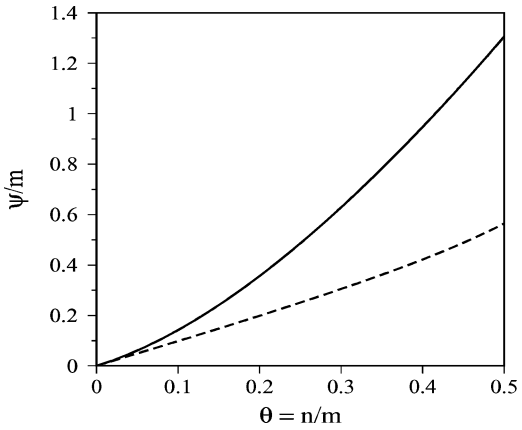

Figure 9. Psi plots for adsorption of pure gases in NaX at 20°C. Solid line: CO_2; dashed line: C_3H_8.

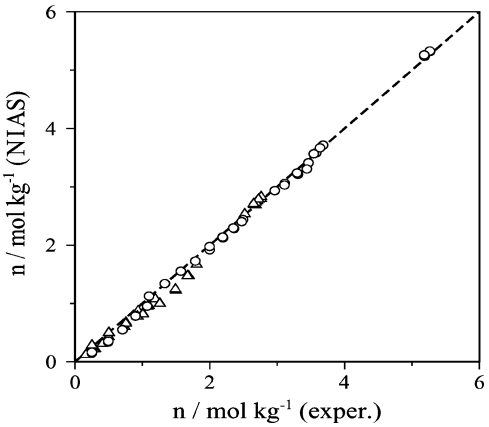

Figure 10. Comparison of NIAS predictions with experiment for binary adsorption in NaX at 20°C. ○: CO_2; △: C_3H_8.

effects are caused by the difference in size of the adsorbate molecules.

Comparison of NIAS with Experiment

Reduced chemicals potentials for adsorption of carbon dioxide and propane in NaX (FAU) are shown on Fig. 9. The large difference in chemical potentials at $\theta = 0.5$ on Fig. 9 ($\delta_{12} = 0.613$) is due to the difference in interaction energies of the two molecules with the exchangeable Na^+ ions: carbon dioxide possesses a large quadrupole moment but propane is nonpolar. NIAS is compared with experiment (Siperstein and Myers, 2001) on Fig. 10. The error in predicting mixture adsorption from single-gas isotherms is reduced from 29.3% for IAS to 9.0% for NIAS.

Summary and Conclusions

Table 1 summarizes a comparison of NIAS predictions with experiment. The mixtures which are in fact ideal are correctly identified by the equality of their ψ plots for the pure components. For nonideal solutions, the NIAS predictions are a considerable improvement over

Table 1. Comparison of NIAS predictions with experiment.

					Error (%)		
Gas 1	Gas 2	Adsorbent	T (K)	δ_{12}	NIAS	IAS	Ref.
CO_2	C_3H_8	NaX (FAU)	293	0.613	9.0	29.3	Siperstein and Myers, 2001
CO_2	C_2H_4	NaX (FAU)	293	0.122	4.8	7.4	Siperstein and Myers, 2001
CO_2	C_2H_6	NaX (FAU)	293	0.613	9.6	17.2	Siperstein and Myers, 2001
C_2H_4	C_2H_6	NaX (FAU)	293	0.217	4.8	13.0	Siperstein and Myers, 2001
SF_6	C_2H_6	NaX (FAU)	293	0.0	4.1	4.1	Siperstein and Myers, 2001
C_2H_6	CH_4	Silicalite (MFI)	293	0.0	3.2	3.2	Siperstein and Myers, 2001
SF_6	CH_4	Silicalite (MFI)	293	0.040	4.9	9.1	Siperstein and Myers, 2001
CO_2	C_3H_8	H-mordenite	303	1.050*	6.6	29.8	Talu and Zwiebel, 1986
H_2S	C_3H_8	H-mordenite	303	1.500*	4.3	34.3	Talu and Zwiebel, 1986
H_2S	CO_2	H-mordenite	303	0.0	11.5	11.5	Talu and Zwiebel, 1986
C_2H_6	C_2H_4	Nuxit AC	293	0.0	1.8	1.8	Szepesy and Illes, 1963

*: cannot be predicted from single-gas isotherms.

IAS predictions. In two cases, Eqs. (17) and (18) fit the experimental data but the value of δ_{12} cannot be determined from the single-gas adsorption isotherms. This complication arises for mixture pairs with large differences in polarity *and* size. Fortunately, the inability of NIAS to predict the δ_{12} constant is apparent in the ψ plots for the pure gases, which intersect at values of pore filling below $\theta = \frac{1}{2}$. Mixtures for which the δ_{12} constant can be predicted have differences in chemical potential which increase smoothly with pore filling as shown on Figs. 5, 7 and 9.

References

Dunne, J. and A.L. Myers, "Adsorption of Gas Mixtures in Micropores: Effect of Difference in Size of Adsorbate Molecules," *Chem. Eng. Science*, **49**, 2941–2951 (1994).

Myers, A.L. "Thermodynamics of Adsorption in Porous Materials," *AIChE J.*, **48**, 145–160 (2002).

Myers, A.L. and J.M. Prausnitz, "Thermodynamics of Mixed-Gas Adsorption," *AIChE J.*, **11**, 121–127 (1965).

Siperstein, F.R. and A.L. Myers, "Mixed-Gas Adsorption," *AIChE J.*, **47**, 1141–1159 (2001).

Szepesy, L. and V. Illes, *Acta Chim. Hung.*, **35**, 245 (1963).

Talu, O. and I. Zwiebel, *AIChE J.*, **32**, 1263 (1986).